Composition of size-resolved aged boreal fire aerosols: Brown carbon, biomass burning tracers, and reduced nitrogen

Robert A. Di Lorenzo[§ʿ], *Bryan K. Place*[§'], *Trevor C. VandenBoer*[†‡], *and Cora J. Young*[*§‡]

[§]Department of Chemistry, Memorial University, St. John's, Newfoundland and Labrador, Canada

[†]Department of Earth Science, Memorial University, St. John's, Newfoundland and Labrador, Canada

KEYWORDS

biomass burning, brown carbon, molecular absorption, alkyl amines, boreal wildfire, size-resolved aerosols, organic aerosol

ABSTRACT

Aerosols that were size-resolved into 13 fractions between 10 nm and 18 μm were collected from an aged boreal forest wildfire plume in July 2013. Samples were extracted into water and analyzed for molecular size-resolved brown carbon (BrC), biomass burning (BB) markers, reduced nitrogen compounds, and elemental composition. Absorption of BrC was primarily in fine-mode aerosols and dominated by high-molecular weight compounds (> 500 Da). The molecular size distribution of BrC was conserved across aerosol sizes, with a decrease in the importance of large molecules in smaller aerosols. The aerosol size-resolved composition of BrC absorption was different than both BB markers, non-sea salt potassium and levoglucosan, suggesting they may not be suitable for identifying BB BrC in aged plumes. Strong correlations were observed between BrC and the reduced nitrogen compounds ammonium, dimethyl amine, and diethyl amine. In aerosols with high BrC and reduced nitrogen, there was a strong cationic excess. These observations could be caused by: i) uptake of ammonium and alkyl amines to form stable salts with organic acids or ii) reactive uptake to form imines or enamines that were hydrolyzed during the BrC extraction process.

INTRODUCTION

Biomass burning (BB) is a major source of organic mass to the atmosphere, second in magnitude only to the atmospheric processing of biogenic volatile organic compounds (BVOCs) to form secondary organic aerosol (SOA).[1] Although much work has gone into mechanistically understanding the BB combustion process[2–4] and characterizing gas- and aerosol-phase molecular markers,[5,6] the majority of BB-derived organics remain uncharacterized. The fraction of these organics that absorb light affect climate and can be sub-divided into two classes: compounds with wavelength-independent absorption that are primarily water-insoluble (black carbon, BC) and compounds with wavelength-dependent absorption that are primarily water soluble (brown carbon,

BrC). The molecular character of BrC is particularly uncertain and has been the subject of numerous studies over the past decade. Although many SOA-mediated formation mechanisms of BrC from biogenic and anthropogenic gas-phase precursors have been proposed (e.g.[7–9]) measurements of real samples demonstrate that BB aerosols are a dominant atmospheric source of BrC.[10–13] Representation of BrC in radiative budget models has been reported to modify an overall negative aerosol radiative forcing (RF) to one that is positive,[14] and to increase the direct radiative effect of all organic aerosol.[15] This exemplifies the uncertainty that persists in our understanding of the cumulative effects of aerosol on global radiative balance. Studies that have included BrC in climate models[16–20] report that accuracy of their predictions is hindered by the large variability of measured BrC absorption efficiencies and uncertain chemical fate.[10,19,14] High molecular-weight species appear to be important to BrC absorption, particularly in aged aerosols.[11,13] Relatively little is known about the sources and fate of these large molecules. Recent in situ measurements indicate that BBOA[21] and BB-derived BrC[10] are externally mixed. Understanding the aerosol size-resolved composition of BB BrC is essential to better constrain BrC sources and fate. To our knowledge, measurements of this type have not yet been made.

Identification of biomass burning organic aerosol (BBOA) is essential for correct source-attribution of BrC. The atmospheric presence of BBOA is typically determined using aerosol (e.g. levoglucosan,[22] potassium[23]) and gas-phase (e.g. carbon monoxide,[24] and acetonitrile[25]) markers or a mass fragment (m/z 60.021, $C_2H_4O_2^+$) associated with levoglucosan and related anhydrosugars.[26] However, the atmospheric lifetime of levoglucosan suggests that it cannot be used to accurately identify aged BBOA.[27,28] Recent evidence also suggests that potassium is externally mixed with the large organic molecules thought to contribute to BrC in a BB plume.[21]

Laboratory experiments and analysis of real samples suggest that reduced nitrogen compounds contribute to BrC.[7,8,29] Nearly 2 Tg of nitrogen are emitted annually in the form of ammonia and methylamines as a result of biomass burning,[30] particularly during smoldering.[24] The reaction of such reduced nitrogen compounds with oxidized organics has been shown to create absorbing moieties for small molecules.[7–9] However, their association with absorbing species of a variety of molecular sizes remains uncharacterized.

This work describes the size-resolved aerosol chemical characterization of several emitted BB species relating to BrC absorption. Specifically, we present i) the aerosol size-resolved composition of molecularly size-resolved BrC, BB tracers potassium and levoglucosan, and reduced nitrogen species; and ii) the relationship of BB tracers and reduced nitrogen to BrC.

EXPERIMENTAL

Sample collection

Samples were collected on July 6, 2013 during a fire plume intrusion into St. John's, Newfoundland and Labrador, Canada. A nano microorifice uniform deposit impactor (nanoMOUDI; model 122-R, MSP Corporation, Shoreview, MN, USA) located in St. John's (47.572°N, 52.722°W, 42 m above sea level) collected aerosol samples onto pre-muffled (500 ^{0}C, 4 hr) aluminum substrates over 25.5 hr at 30 SLPM for a total sample volume of 45.9 m^3. During the same event, a local air quality station measured $PM_{2.5}$ mass loadings up to 120 μg m^{-3} and our group determined a $PM_{2.5}$ water-soluble organic carbon (WSOC) loading of 27 μg m^{-3}.[31] The nanoMOUDI separates aerosols by aerodynamic diameter (D_p) into 13 fractions with size cut-offs (μm) of: 10, 5.6, 3.2, 1.8, 1.0, 0.56, 0.32, 0.18, 0.10, 0.056, 0.032, 0.018, and 0.010. Samples were stored in the dark at -20 ^{0}C prior to extraction. Back trajectory analysis for the same fire and same

85 sampling site indicated the aerosols had transported over the Gulf of St. Lawrence and had aged
86 in the atmosphere for approximately 48 hours (Figure S1).[13]

87 *Brown carbon extraction and analysis*

88 Impactor substrate sub-samples (10 % pie slice) were placed in pre-cleaned glass vials.
89 Samples were sonicated in 750 µL ultrapure deionized water (Barnstead Infinity Ultrapure Water
90 System, Thermo Scientific, Waltham, MA) for 45 minutes at room temperature. Extracts were
91 filtered with 0.2 µm PTFE syringe filters (Iso-Disc, Supelco, Bellefonte, PA, USA) and transferred
92 to pre-cleaned glass sample vials. Injections of 100 µL were made into a high performance liquid
93 chromatography (HPLC) system (1260 Infinity, Agilent Technologies, Santa Clara, CA, USA) and
94 separated using an aqueous gel filtration column (Polysep GFC P-3000, Phenomenex, Torrance,
95 Ca, USA) with a 25-mM aqueous ammonium acetate eluent at a flow rate of 1 mL min^{-1}. Absorbing
96 compounds were detected using a diode array detector (1260, Agilent Technologies, Santa Clara,
97 CA, USA). The initial filter of the nano-MOUDI (stage 0, cut-off diameter ~18 µm) was extracted
98 and treated as a sampling blank. Clean water was injected as an analytical blank. No signal was
99 observed in any blanks. Using a calibration method described previously[31] (details in SI, Figure
100 S2), molecular weights of absorbing compounds were estimated.

101 *Ion chromatography analysis*

102 Ion chromatographic (IC) analysis was performed using a ThermoScientific ICS-2100 Ion
103 Chromatography System. A detailed presentation of the method, performance, and unique
104 capabilities of the cation and alkyl amine analysis method is outlined in Place *et al.*[32] Species that
105 could be quantified by the cation method were: Li^+, Na^+, NH_4^+, K^+, Mg^{2+}, Ca^{2+}, and a suite of up
106 to eleven alkyl amines. The instrument and all related products were obtained from
107 ThermoScientific (Mississauga, ON, Canada). Briefly, 1 mL aqueous samples were injected using

108 an autosampler (AS-DV) and the cations therein preconcentrated on a cation-exchange column
109 (TCC-UPL1, 4 mm x 23 mm). Analytes were separated on a cation exchange analytical column
110 (CS19, 4 mm x 250 mm) with a guard column (CG19, 4 mm x 50 mm) using gradient elution with
111 continuously generated methane sulfonic acid (MSA) as the solvent modifier (EGC II MSA
112 Generator Cartridge). Eluent ions were selectively suppressed (CSRS 300 Ion Supressor, 4mm)
113 before the analytes were measured using conductivity detection (DS6, 30 ºC).

114 Species that could be quantified by the anion method were: F^-, Cl^-, NO_2^-, Br^-, NO_3^-, SO_4^{2-},
115 PO_4^{3-}, and a suite of up to seven organic acids.[33] Anions were also preconcentrated from 1 mL
116 samples (TAC-ULP1, 4 mm x 23 mm) and separated on an anion exchange column (AS19, 4 mm
117 × 250 mm) with a guard column (AG19, 4 mm x 50 mm) using gradient elution with potassium
118 hydroxide (KOH) at a flow rate of 1.5 mL min^{-1}. The separation program held at 1 mM for 7
119 minutes, followed by a linear increase to 16 mM over 9 minutes, held at 16 mM for 4 minutes,
120 increased linearly to 25 mM over the next 5 minutes, then to 60 mM over the next 8 minutes before
121 being returned to the initial conditions to equilibrate prior to the next analytical determination. The
122 KOH eluent was suppressed (AERS 500 Ion Suppressor, 4mm) before the analytes were detected
123 by conductivity (DS6, 30 ºC). Calibration and quality control methods can be found in the SI.

124 *Levoglucosan analysis*

125 Samples were separated using high performance liquid chromatography (HPLC) (1260
126 Infinity, Agilent Technologies, Santa Clara, CA, USA) on a hydrophilic interaction
127 chromatography (HILIC) column (X-Bridge BEH Amide, 2.5 µm x 4.6 mm x 100 mm, Waters
128 Corporation, Milford, MA, USA) with a mobile phase consisting of (A) 0.1% acetic acid in water
129 and (B) acetonitrile. A gradient elution at a flow rate of 0.5 mL min^{-1} was used for the separation
130 of 10 µL injections with the following program: Initial conditions of 10% A were held for 0.1

131 minutes and linearly increased to 80% A over the next 0.9 minutes. This composition was held for
132 5 minutes before conditions were returned to the initial 10% A over 0.1 minutes and allowed to
133 reequilibrate, for a total run time of 10 minutes. Compounds were detected using a time-of-flight
134 mass spectrometer (6230, Agilent Technologies, Santa Clara, CA, USA) with electrospray
135 ionization in positive mode (ESI+) with the following acquisition parameters: capillary voltage:
136 3.5 kV, gas temperature: 350 °C, gas flow: 12 L min^{-1}, nebulizer pressure: 35 psig, and cone
137 voltage of 175 V. Quantification was performed via external calibration using peak areas from
138 extracted ion chromatograms with a 0.002 Da mass window. The sodiated adduct of levoglucosan
139 (m/z = 185.0426) was used for quantification, which eluted at ~ 3 min. The sodiated adduct of
140 methyl β-D-xylopyranoside (m/z = 187.0582) was used as an internal standard to track ionization
141 efficiency. Calibration between 0.1 and 1 μg mL^{-1} was used to quantify levoglucosan in each
142 sample. Calibration was run before and after the sample analysis. Precision in the levoglucosan
143 analysis was determined from 1σ error in the fit coefficients of the linear regression using the
144 calibration standards bracketing the sample range, yielding a maximum error of 5 % in sample
145 quantification.

146 *Elemental analysis*

147 Elemental analysis was undertaken with inductively coupled plasma optical emission
148 spectroscopy (ICP-OES) using an iCap 6500 Series ICP-OES (ThermoScientific, Mississauga,
149 ON, Canada) to quantify Al, Ca, Fe, K, Mg, Mn, Na, P, S, and Si. Samples were acidified to 2%
150 (v/v) HNO_3 prior to analysis. The instrument was calibrated at the start of the analysis, with low
151 and high range check standards and a reagent blank run every 20 samples. Yttrium was added
152 inline as an internal standard. A drift check was performed every 15 samples and re-calibrated if
153 the drift check failed. Each sample was analyzed four times using the following settings: nebulizer

154 pump flush rate: 100 rpm, analysis pump rate: 50 rpm, pump relaxation time: 20 s, RF power: 1150
155 W, nebulizer flow: 0.55 L min^{-1}, auxiliary gas: 0.5 L min^{-1}.
156

157 **RESULTS AND DISCUSSION**

158 *Aerosol size distribution of molecular size-separated BrC*

159 Fine mode aerosols ($0.10 < D_p < 1.0$ μm) contained the largest fraction of BrC, with
160 smaller absorption measured in ultrafine ($0.010 < D_p < 0.10$ μm) and coarse ($1.0 < D_p < 10$ μm)
161 modes (Figure 1A; Tables S1, S2). Maximum absorption was observed between 0.56 and 1.0 μm.
162 Trends were consistent across all wavelengths measured by the diode array. To our knowledge,
163 the only other BrC size-resolved aerosol measurements were made in an urban area not strongly
164 impacted by BB.[34] This urban BrC was also enhanced in the fine mode, with maximum absorption
165 between 0.31 and 1.0 μm.[34] Aerosol size-resolved composition of WSOC, of which BrC is a subset,
166 has been measured in several BB-impacted areas and is also a useful comparison. In the urban BrC
167 measurements described above, maximum BrC absorption coincided with maximum
168 concentrations of organic carbon and WSOC.[35] In agreement with our observations, WSOC is
169 commonly enriched in submicron BB aerosols.[36–38] Peak WSOC was observed between 0.32 and
170 0.56 μm in both laboratory single-species burning experiments[38] and measurements of aged
171 aerosol from a boreal wildfire.[37] Similarly, peak WSOC was between 0.14 and 1.2 μm in the
172 Amazon during dry season.[36] We observed 93 % of the BrC absorption in the fine mode. This is
173 consistent with 92.3 – 97.7 % of the total PM_{10} WSOC in aerosols smaller than 1.8 μm in
174 laboratory studies, depending on the biomass species.[38] Similarly, measurements of aged aerosols
175 emitted from a boreal wildfire showed 77 % of the total PM_{10} WSOC was found in the submicron
176 fraction.[37] For these laboratory and field BB studies, WSOC concentration tracked closely with

177 total aerosol mass loadings.[36–38] Although it would be useful to have size-resolved aerosol mass
178 and WSOC for these samples to compare to previous studies, limited sample mass precluded such
179 measurements. Comparison with these previous studies suggests that aerosol WSOC and BrC is
180 found predominantly in the fine mode for fresh laboratory emissions,[38] field measurements aged
181 between 5 – 36 hours,[37] our measurements in this work aged 48 hours, and urban emissions.[34]

182 The aerosol size distribution of molecular-size-separated absorbing species identified
183 three molecular weight maxima (estimated at 2800 Da, 1800 Da, and ≤ 250 Da). These maxima
184 were conserved across all aerosol sizes (Figure 1B). It should be noted that the maximum at 250
185 Da is a limitation of the chromatographic column. It represents the summed absorbance of
186 compounds ≤ 250 Da, as they all elute simultaneously in the column exclusion volume due to the
187 porosity limit of the stationary phase. Although the molecular size corresponding to absorption
188 maxima were consistent across all aerosol sizes, as aerosol size decreased the fraction of smaller
189 molecular weight absorbers were responsible for an increasing proportion of the total absorption
190 (Figure 1C). For example, small molecules (< 500 Da) accounted for 20 % of the total absorption
191 in the 0.56 – 1.0 μm size bin and 29 % of the total absorption in the 18 – 32 nm size bin. This is
192 consistent with single particle mass spectrometric measurements of sub-micron aerosols showing
193 that smaller molecular weight fractions of BBOA are in greater proportion in smaller diameter
194 aerosols.[39]

195 *Aerosol size distribution of BB markers and relationship to BrC*

196 Several markers are used as proxies for detecting BB influence in aerosol composition,
197 including potassium[23] and levoglucosan.[22] Since source apportionment to BB is typically
198 performed using these markers, it is worthwhile to assess their size distribution. Because the BB
199 plume measured in this study passed over coastal marine regions, our IC measurement of sodium

was used to calculate non-sea salt (nss) potassium that could be attributed to BB emissions (details in SI). Nss-potassium (Figure 2A, Table S3) was found in all size fractions, with most of the mass found in the submicron fraction. The maximum concentration was in the same size bin as maximum BrC absorption, between 0.56 and 1.0 μm. Aerosol diameter-normalized mass loadings for nss-potassium ranged between 0.03 – 0.74 μg m^{-3}. A bimodal distribution was observed with a second maximum in the ultrafine mode, between 18 and 32 nm. Previous studies have observed higher loadings of potassium between 0.44 and 1.2 μm.[36,40] Differences between fires are expected as potassium emissions from BB are known to be dependent on fire conditions[26] and fuel type.[38] Levoglucosan (Figure 2B, Table S3) was found in all size fractions and was distributed bimodally, with maxima in the 32 – 56 nm and 0.56 – 1. 0 μm size bins, but its presence extended well into the coarse mode. Aerosol diameter-normalized mass loadings ranged between 0.06 – 0.34 μg m^{-3}. Previous studies have observed levoglucosan primarily in submicron aerosols[40–42] and have reported that its size distribution in submicron aerosol varies with BB source.[40,42] In a recent study, Zhou *et al.* observed that low incidence of the BBOA marker (m/z 60) in known BB aerosols could cause mis-assignment of aged BBOA.[28]

Understanding the relationship between the size distribution of BrC and BB markers is important for correct BrC source apportionment. We show the strength of the linear relationship between small (< 500 Da) and large (> 500 Da) BrC absorption with the quantities of BB markers for all aerosol sizes and each aerosol mode (Table 1, Figure S3). When including all aerosol size bins, correlations between nss-potassium and large- (r^2 = 0.59) and small-molecule (r^2 = 0.59) BrC absorption were moderate. This is similar to laboratory studies[38] and field measurements from the Amazon Basin[36] that observed moderate to strong correlations between aerosol size-resolved potassium and WSOC from BB across all size bins.[36] The strength of our observed relationships

223 changed, showing a dependence on aerosol size. All nss-potassium-BrC correlations were positive
224 and strong for coarse- and fine-mode aerosols ($0.85 \leq r^2 \leq 0.97$), while positive correlations in
225 ultrafine-mode aerosols were moderate for both small- ($r^2 = 0.55$) and large-molecule ($r^2 = 0.52$)
226 BrC absorption. Slopes for the linear relationships were different for each aerosol mode. This
227 suggests the possibility of non-uniform mixing of nss-potassium and BrC in the BB aerosol
228 population. Laboratory measurements have shown that aerosol potassium and organics are formed
229 through different mechanisms and are externally mixed in fresh BB aerosols.[43] Single particle mass
230 spectrometer measurements of an aged BB plume with higher D_p resolution than our measurements
231 have shown that potassium distributions have a modal maximum ~100 nm smaller than BBOA.[39]

232 Positive correlations between levoglucosan and BrC absorption when including all
233 aerosol size bins were weak for both small ($r^2 = 0.32$) and large ($r^2 = 0.30$) molecules. Strong
234 positive correlations were observed between BrC absorption and levoglucosan only in the fine
235 mode ($r^2 \geq 0.87$), while weak and very weak correlations characterized the relationships in the
236 coarse ($r^2 \leq 0.39$) and ultrafine ($r^2 \leq 0.12$) modes with slopes close to zero. These distributions
237 highlight the importance of understanding aerosol mixing when assessing the quality of a
238 molecular marker, especially in bulk or time-integrated aerosol samples. The need for more single
239 particle and size resolved aerosol measurements is apparent.

240 *Aerosol size distribution of reduced nitrogen and relationship to BrC*

241 Reduced nitrogen species, including ammonium and alkyl amines, were elevated in the
242 aged BB plume (Figure S4, Table S3). Mass loading data for these reduced nitrogen species was
243 reported in Place *et al.*[32] and is briefly summarized here. The sum of two alkyl amines,
244 dimethylamine (DMA) and diethylamine (DEA), dominated the total mass and molar composition
245 of this compound class across all size bins. The size distribution was similar for all detected

246 reduced nitrogen compounds (Figure 3), with detectable levels in all size fractions between 0.032
247 and 3.2 μm. DEA and DMA were highest in the 0.32 – 0.56 μm size bin, while ammonium was
248 highest in the 0.56 – 1.0 μm size bin. Alkyl amines have been detected in BB aerosols in several
249 studies,[32,44] but always at levels lower than ammonium by one to three orders of magnitude.[45] This
250 is consistent with previous measurements of 10 – 15-hour aged BB aerosols made with the same
251 reduced nitrogen analysis technique used herein.[32] The summed alkyl amine molar concentration
252 in those samples was approximately 10 % of ammonium. In the current samples, mass
253 concentrations of DEA exceeded those of ammonium in all size bins, while the molar
254 concentration of DEA exceeded ammonium in two size bins. This suggests the alkyl amines may
255 be derived from another source and were possibly introduced during atmospheric transport and
256 aging of the BB aerosols. Terrestrial sources of alkyl amines include animal husbandry, food-
257 processing industries, composting operations, and sewage. Since the plume transported across
258 remote Boreal Canadian forest and coastal marine areas, these terrestrial sources can be excluded.
259 However, the coastal marine environment is another known source of amines, where DMA and
260 DEA observed in marine aerosols suggest a common gaseous source.[46–48] Calculated back-
261 trajectories indicated the sampled BB plume mixed with air that passed over the Gulf of St.
262 Lawrence and that the plume was transported directly over coastal regions before being sampled
263 (Figure S1). Alkyl amines have been observed to increase moving from the open ocean to the coast
264 in regions (i.e. coastal upwelling) and/or in areas with high biological activity (i.e. algal blooms).[48–
265 50] Measurements of plankton fluorescence by NASA satellites MODIS-Aqua and Giovanni show
266 oceanic biological activity in the Gulf of St. Lawrence and North Atlantic peaking in May, but
267 also present with high intensity in coastal zones during plume transport. In all known ocean

emission measurements of alkyl amines, DMA and DEA are present at levels 2 – 3 orders of magnitude lower than ammonium.[45]

The abundance of reduced nitrogen in these samples results in cationic excess by molar equivalents charge balance of all measured ionic species in the size bins ranging from 0.18 – 1.0 μm (Figure 4). Our calculation of charge balance includes all nss species (ammonium, alkyl amines, nss-potassium, nss-calcium, nss-magnesium, nss-nitrate, nss-sulfate, organic acids). In the aerosols between 0.56 and 1.0 μm, the charge balance ratio (Σ+/Σ-) exceeds two. Cationic excesses have been observed for BB aerosol previously when calculating charge balance using only sulfate, nitrate, and ammonium.[28,37] Using the same approach as these previous works, we also observe cationic excess in aerosols in the 0.56 – 1.0 μm size fraction. This excess could be related to strong correlations with BrC absorption. The three most abundant reduced nitrogen species correlated strongly with the occurrence of BrC absorption (Table 1, Figure S5). When including all size bins, positive correlations between BrC absorption and all three reduced nitrogen species were strong ($r^2 \geq 0.76$) and statistically significant ($p < 0.001$). Correlations were strongest for ammonium ($r^2 \geq 0.90$), and stronger for large- ($r^2 \geq 0.94$) compared to small-molecule ($r^2 \geq 0.90$) BrC absorbers. Overall, correlations were much stronger between BrC and reduced nitrogen than with the traditional BB markers described above. Slopes of the linear relationships for ammonium with BrC absorption were positive and similar in value, independent of aerosol mode. Positive slopes of the relationships with alkyl amines were consistent for the ultrafine and fine modes, and across all aerosol size bins, but different for the coarse mode. We expect this is caused by low amine signal in the coarse mode but could suggest this mode represents a different aerosol population. Given the general strong association between reduced nitrogen and BrC absorption, two possible explanations could account for the trends. The first possible explanation involves the abundance

291 of carboxylate groups observed in BBOA samples.[21,28,36,51] Ammonium and alkyl amines could
292 form stable salts with carboxylates. It is well known that ammonia[52] and alkyl amines[53] can be
293 taken up into acid-containing aerosols, so reduced nitrogen species may preferentially partition
294 into aerosols already containing BrC. Alkyl amines are more basic than ammonia, which could
295 lead to preferential uptake.[53] A second possible explanation involves reactive uptake of reduced
296 nitrogen. Reactions between carbonyls and ammonia or primary amines form absorbing imines,
297 which may contribute to the absorption of atmospheric BrC.[7–9,54] Similarly, carbonyls can react
298 with secondary amines to form enamines.[9] BB aerosol has been shown to be rich in carbonyls.[51]
299 Imines and enamines would likely be hydrolysed under our extraction conditions yielding the
300 detected reduced nitrogen species. The reformed carbonyls or large molecular mass carboxylates
301 from such hydrolysis would not be detected by the charge balance ratio analytical techniques.
302 Regardless, if these reactions were occurring, they would increase the conjugation of the reduced
303 nitrogen-reacted BrC and the integrated total absorption, such that our BrC measurements reported
304 here would represent a lower-limit of integrated BrC absorption. We cannot distinguish between
305 these two possible explanations using this dataset.
306

307 **CONCLUSIONS**

308 We measured the composition of size-resolved aerosols from a ~48-hour aged biomass burning
309 plume originating from the Canadian boreal forest that transited over marine coastal areas.
310 Measurements by SEC-UV demonstrated that most BrC absorption was in the fine mode,
311 dominated by large-molecule (> 500 Da) absorbers. The molecular size profiles showed three
312 maxima at 2800, 1800, and ≤ 250 Da, which were conserved across aerosol size modes and
313 absorption wavelengths. The proportion of small molecular absorbers increased with decreasing

aerosol size. Both nss-potassium and levoglucosan were externally mixed with aerosols containing BrC absorbers. This suggests these BB markers may not be appropriate indicators of BB origin for BrC and that alternative markers should be sought. Correlations between BrC absorption and reduced nitrogen species ammonium, DMA, and DEA were much stronger than for traditional BB tracers. This was also associated with cationic excess, which could be caused by the formation of stable salts or reactive uptake. Although BB and marine environments are both known sources of amines, the source of these elevated levels of amines is not known. Measurements of ambient aerosol- and gas-phase amines are sparse, making the importance of these interactions highly uncertain. Study of the potential reactivity between BB-generated large molecular weight chromophores and reduced nitrogen compounds and any influence on absorption is warranted. Additional field measurements of BrC from BB, along with gas- and aerosol-phase reduced nitrogen would also aid in elucidating any relationships.

FIGURES

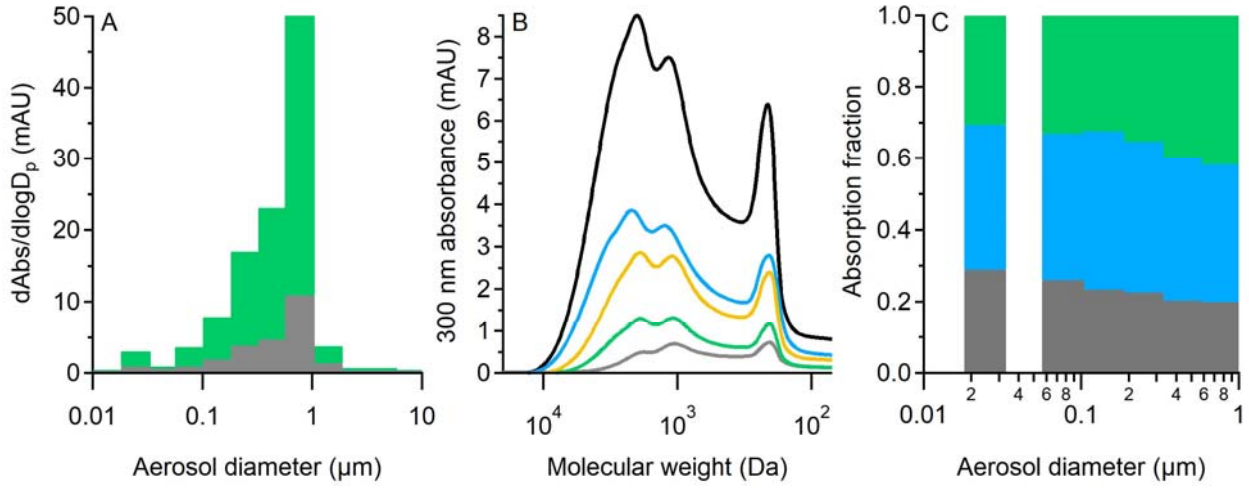

Figure 1. (A) Aerosol size distributions of BrC absorption at 300 nm by (green) molecules larger than 500 Da and (grey) molecules less than 500 Da (traces are stacked to reflect total absorption

at each size fraction BrC); (B) molecular size distribution across aerosol stages as measured using SEC-UV for median aerosol sizes 1.4 µm (grey), 0.78 µm (black), 0.44 µm (blue), 0.25 µm (orange), and 0.14 µm (green); (C) absolute contribution to total absorption for molecules >1800 Da (green), between 1800 and 500 Da (blue), and <500 Da (grey) as a function of aerosol diameter.

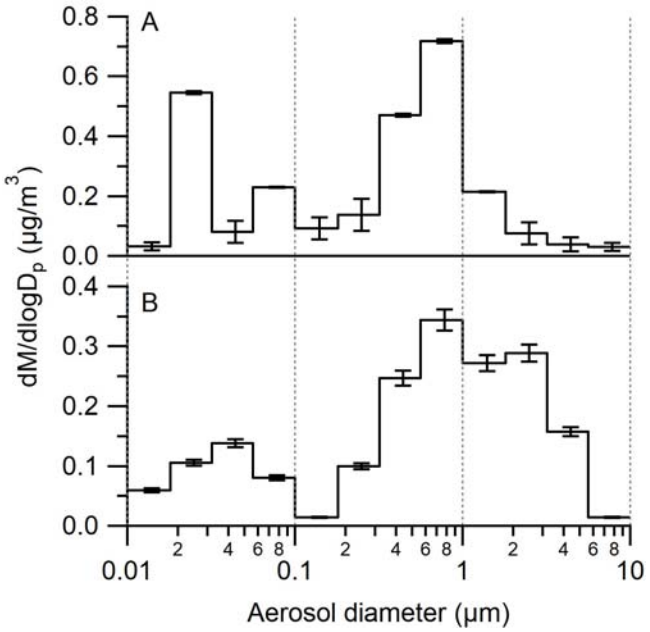

Figure 2. Biomass burning plume aerosol mass loading size distributions of markers (A) potassium and (B) levoglucosan. Error bars indicate: (A) accuracy of the IC measurement (described in Place *et al.*[32]) and (B) 5 % precision error of the LC-MS measurement.

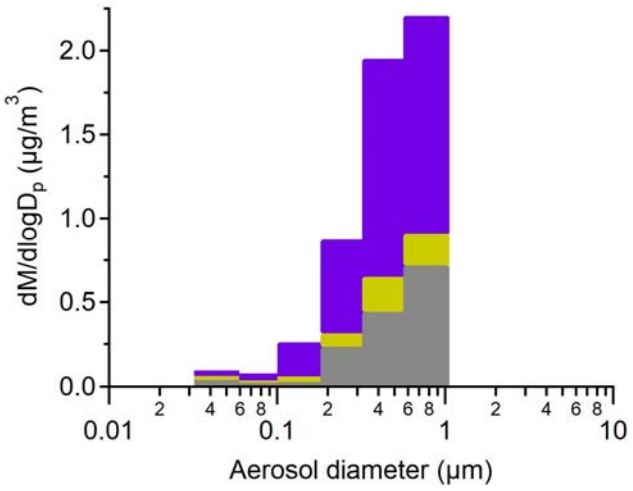

Figure 3. Sum of aerosol mass loading size distributions of the most abundant reduced nitrogen species, with fractional contributions of diethylamine (DEA, purple), dimethylamine (DMA, yellow), and ammonium (grey).

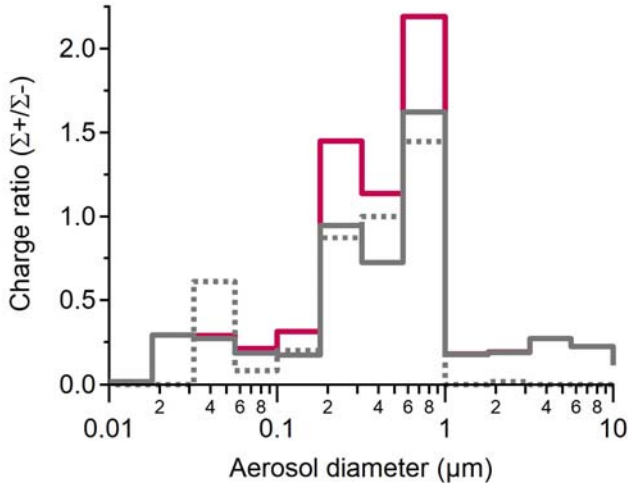

Figure 4. Aerosol size distribution of the mole equivalents charge balance ratio showing: all non-sea salt (nss) charged species (solid red); nss charged species excluding alkyl amines (solid grey); and ammonium, nss-sulfate, nss-nitrate (dashed grey).

TABLES.

Table 1. Linear correlation slope (± standard deviation), coefficient of determination (r^2), and statistical significance (p, 2-tailed) between molecular-size-resolved BrC and biomass burning tracers for all aerosol sizes (n = 12 stages), coarse, fine, and ultrafine modes (each n = 4 stages). None/very weak ($r^2 < 0.3$), weak ($0.3 \leq r^2 < 0.5$), moderate ($0.5 \leq r^2 < 0.7$), and strong ($r^2 \geq 0.7$) shown in grey, black, purple, and red, respectively. Statistically significant correlations ($p \leq 0.05$) shown in bold. Correlations were only performed if at least three stages had loadings greater than the detection limit of the analytical method.

		< 500 Da			> 500 Da		
		m	r^2	p	m	r^2	p
Non-sea salt potassium	Total	**10 ± 3**	**0.59**	**0.003**	**40 ± 10**	**0.59**	**0.003**
	Ultrafine	1.2 ± 0.8	0.55	0.213	4 ± 3	0.52	0.240
	Fine	**12 ± 4**	**0.85**	**0.045**	**50 ± 10**	**0.89**	**0.026**
	Coarse	**6.3 ± 0.8**	**0.97**	**0.004**	**13 ± 2**	**0.95**	**0.009**
Levoglucosan	Total	16 ± 7	0.32	0.052	57 ± 30	0.30	0.065
	Ultrafine	4 ± 7	0.12	0.645	-4 ± 28	0.01	0.900
	Fine	24 ± 8	0.82	0.058	**90 ± 20**	**0.87**	**0.034**
	Coarse	3 ± 2	0.39	0.338	5 ± 5	0.26	0.461
Ammonium	Total	**13 ± 1**	**0.94**	**<0.001**	**50 ± 3**	**0.97**	**<0.001**
	Ultrafine	–	–	–	–	–	–
	Fine	**13 ± 3**	**0.90**	**0.023**	**47 ± 8**	**0.94**	**0.011**
	Coarse	–	–	–	–	–	–
Dimethyl amine	Total	**0.036 ± 0.006**	**0.76**	**<0.001**	**0.14 ± 0.02**	**0.81**	**<0.001**
	Ultrafine	–	–	–	–	–	–
	Fine	0.03 ± 0.02	0.48	0.269	0.12 ± 0.08	0.55	0.213
	Coarse	**0.4 ± 0.1**	**0.88**	**0.031**	**0.9 ± 0.1**	**0.96**	**0.007**
Diethyl amine	Total	**0.0056 ± 0.0009**	**0.81**	**<0.001**	**0.022 ± 0.003**	**0.85**	**<0.001**
	Ultrafine	0.006 ± 0.008	0.21	0.523	0.01 ± 0.03	0.08	0.707
	Fine	0.005 ± 0.003	0.57	0.200	0.02 ± 0.01	0.65	0.151
	Coarse	**0.041 ± 0.008**	**0.93**	**0.013**	**0.087 ± 0.009**	**0.98**	**0.003**

ASSOCIATED CONTENT

Supporting Information: contains three figures relevant to the results and discussion and three tables of raw data from all measurements (file type, PDF)

AUTHOR INFORMATION

Corresponding Author

* youngcj@yorku.ca OR York University, 4700 Keele Street, Toronto, ON, M3J 1P3

Present Addresses

[ς]Now at: SCIEX, Boston, Massachusetts, USA

[‡]Now at: Department of Chemistry, York University, Toronto, Ontario, Canada

[ˈ]Now at: Department of Chemistry, University of California Berkeley, California, USA

ACKNOWLEDGMENT

We thank Joseph Bautista for sample collection and Jamie Warren for ion chromatography support. Funding was provided by Natural Sciences and Engineering Research Council of Canada through Discovery and Research, Tools, and Infrastructure Grants. TCV acknowledges a Banting Postdoctoral Fellowship.

TABLE OF CONTENTS ART

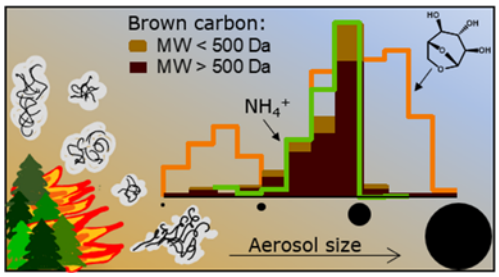

REFERENCES

(1) Boucher, O.; Randall, D.; Artaxo, P.; Bretherton, C.; Feingold, G.; Forster, P. M.;

Kerminen, V.-M.; Kondo, Y.; Liao, H.; Lohmann, U.; et al. Clouds and Aerosols. In *Climate Change 2013: The Physical Science Basis. Contribution of Working Group I to the Fifth Assessment Report of the Intergovernmental Panel on Climate Change*; Stocker, T. F., Qin, D., Plattner, G.-K., Tignor, M., Allen, S. K., Boschung, J., Nauels, A., Xia, Y., Bex, V., Midgley, P. M., Eds.; Cambridge University Press: Cambridge, United Kingdom and New York, NY, USA, 2013.

(2) Roberts, A. F. A review of kinetics data for the pyrolysis of wood and related substances. *Combust. Flame* **1970**, *14* (2), 261–272.

(3) Alger, R. Pyrolysis and Combustion of Cellulosic Materials. In *The Mechanisms of Pyrolysis, Oxidation, and Burning of Organic Materials*; Wall, L. A., Ed.; National Bureau of Standards Special Publication: Washington, D.C., 1972; pp 171–184.

(4) Shafizadeh, F. The Chemistry of Pyrolysis and Combustion. In *The Chemistry of Solid Wood*; American Chemical Society: Washington, D.C., 1984; pp 489–529.

(5) Simoneit, B. R. T. Biomarker PAHs in the Environment. In *PAHs and Related Compounds*; Neilson, A. H., Ed.; Springer Berlin Heidleberg: Berlin, Heidelberg, 1998; Vol. 3, pp 175–221.

(6) Oros, D. R.; Simoneit, B. R. T. Identification and emission factors of molecular tracers in organic aerosols from biomass burning Part 2 . Deciduous trees. *Appl. Geochemistry* **2001**, *16*, 1513–1544.

(7) Shapiro, E. L.; Szprengiel, J.; Sareen, N.; Jen, C. N.; Giordano, M. R.; McNeill, V. F. Light-absorbing secondary organic material formed by glyoxal in aqueous aerosol mimics. *Atmos.*

Chem. Phys. **2009**, *9*, 2289–2300.

(8) Lee, A. K. Y.; Zhao, R.; Li, R.; Liggio, J.; Li, S. M.; Abbatt, J. P. D. Formation of light absorbing organo-nitrogen species from evaporation of droplets containing glyoxal and ammonium sulfate. *Environ. Sci. Technol.* **2013**, *47* (22), 12819–12826.

(9) Aiona, P. K.; Lee, H. J.; Lin, P.; Heller, F.; Laskin, A.; Laskin, J.; Nizkorodov, S. A. A role for 2-methyl pyrrole in the browning of 4-oxopentanal and limonene secondary organic aerosol. *Environ. Sci. Technol.* **2017**, *51* (19), 11048–11056.

(10) Lack, D. A.; Langridge, J. M.; Bahreini, R.; Cappa, C. D.; Middlebrook, A. M.; Schwarz, J. P. Brown carbon and internal mixing in biomass burning particles. *Proceedings of the National Academy of Sciences*. September 2012, pp 14802–14807.

(11) Forrister, H.; Liu, J.; Scheuer, E.; Dibb, J.; Ziemba, L.; Thornhill, K. L.; Anderson, B.; Diskin, G.; Perring, A. E.; Schwarz, J. P.; et al. Evolution of brown carbon in wildfire plumes. *Geophys. Res. Lett.* **2015**, *42*, 4623–4630.

(12) Washenfelder, R. A.; Attwood, A. R.; Brock, C. A.; Guo, H.; Xu, L.; Weber, R. J.; Ng, N. L.; Allen, H. M.; Ayres, B. R.; Baumann, K.; et al. Biomass burning dominates brown carbon absorption in the rural southeastern United States. *Geophys. Res. Lett.* **2015**, *42*, 653–644, doi:10.1002/2014GL062444.

(13) Di Lorenzo, R. A.; Washenfelder, R. A.; Attwood, A. R.; Guo, H.; Xu, L.; Ng, N. L.; Weber, R. J.; Baumann, K.; Edgerton, E.; Young, C. J. Molecular size separated brown carbon absorption for fresh and aged biomass burning plumes at multiple field sites. *Environ. Sci. Technol.* **2017**, *51*, 3128–3137.

(14) Saleh, R.; Marks, M.; Heo, J.; Adams, P. J.; Donahue, N. M.; Robinson, A. L. Contribution of brown carbon and lensing to the direct radiative effect of carbonaceous aerosols from biomass and biofuel burning emissions. *J. Geophys. Res. Atmos.* **2015**, *120*, 10285–10296.

(15) Wang, X.; Heald, C. L.; Liu, J.; Weber, R. J.; Campuzano-jost, P.; Jose, L.; Schwarz, J. P.; Perring, A. E. Exploring the observational constraints on the simulation of brown carbon. *Atmos. Chem. Phys.* **2018**, *18*, 635–653.

(16) Lin, G.; Penner, J. E.; Flanner, M. G.; Sillman, S.; Xu, L.; Zhou, C. Radiative forcing of organic aerosol in the atmosphere and on snow: Effects of SOA and brown carbon. *J. Geophys. Res. Atmos.* **2014**, *119*, 7453–7476.

(17) Jacobson, M. Z. Investigating cloud absorption effects: Global absorption properties of black carbon, tar balls, and soil dust in clouds and aerosols. *J. Geophys. Res. Atmos.* **2012**, *11* (D6).

(18) Jacobson, M. Z. Effects of biomass burning on climate, accounting for heat and moisture fluxes, black and brown carbon, and cloud absorption effects. *J. Geophys. Res. Atmos.* **2014**, *119*, 8980–9002.

(19) Wang, X.; Heald, C. L.; Ridley, D. A.; Schwarz, J. P.; Spackman, J. R.; Perring, A. E.; Coe, H.; Liu, D. Exploiting simultaneous observational constraints on mass and absorption to estimate the global direct radiative forcing of black carbon and brown carbon. *Atmos. Chem. Phys.* **2014**, *14*, 10989–11010.

(20) Feng, Y.; Ramanathan, V.; Kotamarthi, V. R. Brown carbon : a significant atmospheric absorber of solar radiation? *Atmos. Chem. Phys.* **2013**, *13*, 8607–8621.

(21) Lee, A. K. Y.; Willis, M. D.; Healy, R. M.; Wang, J. M.; Jeong, C. H.; Wenger, J. C.; Evans, G. J.; Abbatt, J. P. D. Single-particle characterization of biomass burning organic aerosol (BBOA): Evidence for non-uniform mixing of high molecular weight organics and potassium. *Atmos. Chem. Phys.* **2016**, *16* (9), 5561–5572.

(22) Simoneit, B. R. T.; Schauer, J. J.; Nolte, C. G.; Oros, D. R.; Elias, V. O.; Fraser, M. P.; Rogge, W. F.; Cass, G. R. Levoglucosan, a tracer for cellulose in biomass burning and atmospheric particles. *Atmos. Environ.* **1999**, *33*, 173–182.

(23) Stevens, R. K. Sampling and analysis methods for use in source apportionment studies to determine impact of wood burning on fine particle mass. *Environ. Int.* **1985**, *11*, 271–283.

(24) Yokelson, R. J.; Susott, R.; Ward, D. E.; Reardon, J.; Griffith, D. W. T. Emissions from smoldering combustion of biomass measured by open-path Fourier transform infrared spectroscopy. *J. Geophys. Res.* **1997**, *102* (D15), 18865.

(25) Andreae, M. O.; Merlet, P. Emission of trace gases and aerosols from biomass burning. *Global Biogeochem. Cycles* **2001**, *15* (4), 955–966.

(26) Lee, T.; Sullivan, A. P.; MacK, L.; Jimenez, J. L.; Kreidenweis, S. M.; Onasch, T. B.; Worsnop, D. R.; Malm, W.; Wold, C. E.; Hao, W. M.; et al. Chemical smoke marker emissions during flaming and smoldering phases of laboratory open burning of wildland fuels. *Aerosol Sci. Technol.* **2010**, *44* (9), i–v.

(27) Hennigan, C. J.; Sullivan, A. P.; Collett, J. L.; Robinson, A. L. Levoglucosan stability in biomass burning particles exposed to hydroxyl radicals. *Geophys. Res. Lett.* **2010**, *37* (9), 2–5.

(28) Zhou, S.; Collier, S.; Jaffe, D. A.; Briggs, N. L.; Hee, J.; Iii, A. J. S.; Kleinman, L.; Onasch, T. B.; Zhang, Q. Regional influence of wildfires on aerosol chemistry in the western US and insights into atmospheric aging of biomass burning organic aerosol. *Atmos. Chem. Phys.* **2017**, *17* (3), 2477–2493.

(29) Wang, Y.; Hu, M.; Lin, P.; Guo, Q.; Wu, Z.; Li, M.; Zeng, L.; Song, Y.; Zeng, L.; Wu, Y.; et al. Molecular characterization of nitrogen-containing organic compounds in humic-like substances emitted from straw residue burning. *Environ. Sci. Technol.* **2017**, *51*, 5951–5961.

(30) Lobert, J. M.; Scharffe, D. H.; Hao, W. M.; Crutzen, P. J. Importance of biomass burning in the atmospheric budgets of nitrogen-containing gases. *Nature* **1990**, *346* (6284), 552–554.

(31) Di Lorenzo, R. A.; Young, C. J. Size separation method for absorption characterization in brown carbon: Application to an aged biomass burning sample. *Geophys. Res. Lett.* **2016**, *43* (1), 458–465.

(32) Place, B. K.; Quilty, A. T.; Di Lorenzo, R. A.; Ziegler, S. E.; VandenBoer, T. C. Quantitation of 11 alkylamines in atmospheric samples: Separating structural isomers by ion chromatography. *Atmos. Meas. Tech.* **2017**, *10* (3), 1061–1078.

(33) Place, B. K.; Young, C. J.; Ziegler, S. E.; Edwards, K. A.; Vandenboer, T. C. Passive sampling capabilities for ultra-trace quantitation of atmospheric nitric acid (HNO3) in remote environments. *Atmos. Environ.* **2017**, Submitted.

(34) Liu, J.; Bergin, M.; Guo, H.; King, L.; Kotra, N.; Edgerton, E.; Weber, R. J. Size-resolved

measurements of brown carbon in water and methanol extracts and estimates of their contribution to ambient fine-particle light absorption. *Atmos. Chem. Phys.* **2013**, *13*, 12389–12404.

(35) Liu, W. J.; Li, W. W.; Jiang, H.; Yu, H. Q. Fates of Chemical Elements in Biomass during Its Pyrolysis. *Chem. Rev.* **2017**, *117* (9), 6367–6398.

(36) Fuzzi, S.; Decesari, S.; Facchini, M. C.; Cavalli, F.; Emblico, L.; Mircea, M.; Andreae, M. O.; Trebs, I.; Hoffer, A.; Guyon, P.; et al. Overview of the inorganic and organic composition of size-segregated aerosol in Rondônia, Brazil, from the biomass-burning period to the onset of the wet season. *J. Geophys. Res. Atmos.* **2007**, *112* (1), D01201.

(37) Saarnio, K.; Aurela, M.; Timonen, H.; Saarikoski, S.; Teinilä, K.; Mäkelä, T.; Sofiev, M.; Koskinen, J.; Aalto, P. P.; Kulmala, M.; et al. Chemical composition of fine particles in fresh smoke plumes from boreal wild-land fires in Europe. *Sci. Total Environ.* **2010**, *408* (12), 2527–2542.

(38) Park, S.-S.; Sim, S. Y.; Bae, M.-S.; Schauer, J. J. Size distribution of water-soluble components in particulate matter emitted from biomass burning. *Atmos. Environ.* **2013**, *73*, 62–72.

(39) Lee, A. K. Y.; Willis, M. D.; Healy, R. M.; Wang, J. M.; Jeong, C.-H.; Wenger, J. C.; Evans, G. J.; Abbatt, J. P. D. Single particle characterization of biomass burning organic aerosol (BBOA): evidence for non-uniform mixing of high molecular weight organics and potassium. *Atmos. Chem. Phys. Discuss.* **2015**, *15* (22), 32157–32183.

(40) Zhang, Z.; Gao, J.; Engling, G.; Tao, J.; Chai, F.; Zhang, L.; Zhang, R.; Sang, X.; Chan, C.

Y.; Lin, Z.; et al. Characteristics and applications of size-segregated biomass burning tracers in China's Pearl River Delta region. *Atmos. Environ.* **2015**, *102* (101), 290–301.

(41) Schkolnik, G.; Falkovich, A. H.; Rudich, Y.; Maenhaut, W.; Artaxo, P. New analytical method for the determination of levoglucosan, polyhydroxy compounds, and 2-methylerythritol and its application to smoke and rainwater samples. *Environ. Sci. Technol.* **2005**, *39* (8), 2744–2752.

(42) Herckes, P.; Engling, G.; Kreidenweis, S. M.; Collett, J. L. Particle size distributions of organic aerosol constituents during the 2002 yosemite aerosol characterization study. *Environ. Sci. Technol.* **2006**, *40* (15), 4554–4562.

(43) Torvela, T.; Tissari, J.; Sippula, O.; Kaivosoja, T.; Leskinen, J.; Virén, A.; Lähde, A.; Jokiniemi, J. Effect of wood combustion conditions on the morphology of freshly emitted fine particles. *Atmos. Environ.* **2014**, *87*, 65–76.

(44) Maudlin, L. C.; Wang, Z.; Jonsson, H. H.; Sorooshian, A. Impact of wildfires on size-resolved aerosol composition at a coastal California site. *Atmos. Environ.* **2015**, *119*, 59–68.

(45) Ge, X.; Wexler, A. S.; Clegg, S. L. Atmospheric amines - Part I. A review. *Atmos. Environ.* **2011**, *45* (3), 524–546.

(46) Facchini, M. C.; Decesari, S.; Rinaldi, M.; Carbone, C.; Finessi, E.; Mircea, M.; Fuzzi, S.; Moretti, F.; Tagliavini, E.; Ceburnis, D.; et al. Important Source of Marine Secondary Organic Aerosol from Biogenic Amines. *Environ. Sci. Technol.* **2008**, *42* (24), 9116–9121.

(47) Müller, C.; Iinuma, Y.; Karstensen, J.; van Pinxteren, D.; Lehmann, S.; Gnauk, T.;

Herrmann, H. Seasonal variation of aliphatic amines in marine sub-micrometer particles at the Cape Verde islands. *Atmos. Chem. Phys. Discuss.* **2009**, *9* (4), 14825–14855.

(48) Youn, J. S.; Crosbie, E.; Maudlin, L. C.; Wang, Z.; Sorooshian, A. Dimethylamine as a major alkyl amine species in particles and cloud water: Observations in semi-arid and coastal regions. *Atmos. Environ.* **2015**, *122*, 250–258.

(49) Sorooshian, A.; Padro, L. T.; Nenes, A.; Feingold, G.; McComiskey, A.; Hersey, S. P.; Gates, H.; Jonsson, H. H.; Miller, S. D.; Stephens, G. L.; et al. On the link between ocean biota emissions, aerosol, and maritime clouds: Airborne, ground, and satellite measurements off the coast of California. *Global Biogeochem. Cycles* **2009**, *23* (4), 1–15.

(50) Gibb, S. W.; Mantoura, R. F. C.; Liss, P. S. Ocean-atmosphere exchange and atmospheric speciation of ammonia and methylamines in the region of the NW Arabian Sea. *Global Biogeochem. Cycles* **1999**, *13* (1), 161–178.

(51) Russell, L. M.; Bahadur, R.; Ziemann, P. J. Identifying organic aerosol sources by comparing functional group composition in chamber and atmospheric particles. *Proc. Natl. Acad. Sci.* **2011**, *108* (9), 3516–3521.

(52) Dinar, E.; Anttila, T.; Rudich, Y. Article CCN Activity and Hygroscopic Growth of Organic Aerosols Following Reactive Uptake of Ammonia CCN Activity and Hygroscopic Growth of Organic Aerosols Following Reactive Uptake of Ammonia. **2008**, *42* (3), 793–799.

(53) Barsanti, K. C.; McMurry, P. H.; Smith, J. N. The potential contribution of organic salts to new particle growth. *Atmos. Chem. Phys.* **2009**, *9*, 2949–2957.

(54) De Haan, D. O.; Hawkins, L. N.; Welsh, H. G.; Pednekar, R.; Casar, J. R.; Pennington, E.

A.; De Loera, A.; Jimenez, N. G.; Symons, M. A.; Zauscher, M.; et al. Brown carbon production in ammonium- or amine-containing aerosol particles by reactive uptake of methylglyoxal and photolytic cloud cycling. *Environ. Sci. Technol.* **2017**, *51* (13), 7458–7466.